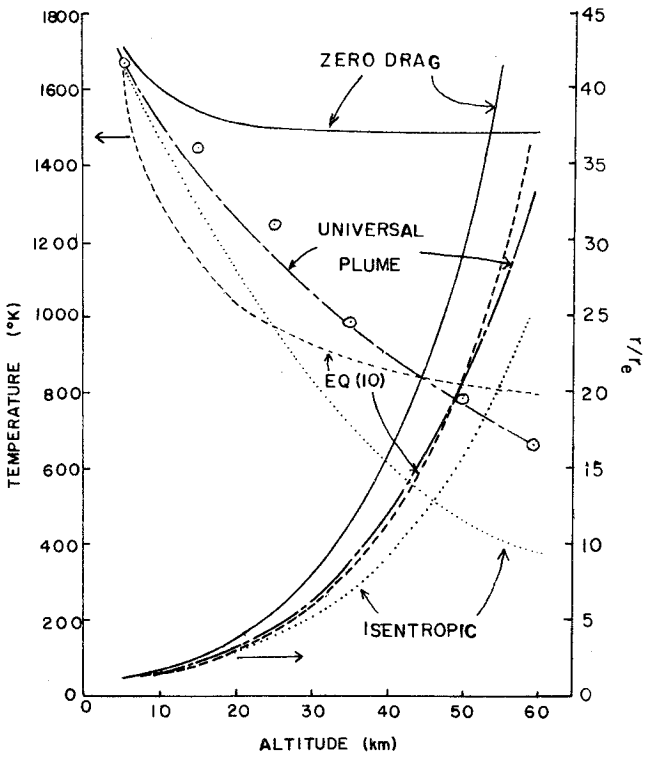

Fig. 4 Prediction of temperature and radius ratio at matched pressure location: ···, isentropic expansion; ——, zero drag; —— –, universal plume drag; ---, Eq. (10); ⊙ Wilson's predictions.

in the figure are temperature predictions reported by Wilson [10] using a more complete, though still approximate, method for calculating the expansion region. That method includes the plume shock, Mach disk, and reflected shock, although approximately. That the technique described here, using a drag coefficient based on the universal plume shape, is in excellent agreement with the more complex model indicates that the present model for C_D does account for the entropy production within the expansion region.

IV. Conclusions

A mathematical model for a low altitude plume which assumes that the plume is at constant pressure is limited, to a large extent, by the accuracy of the input conditions for the model: the temperature, concentrations, velocity, and size of the plume at the matched pressure point. Integral balances of mass, momentum, and energy can be employed to solve for these input conditions. A method of prescribing a drag coefficient has been identified which has three favorable attributes: it is extremely easy to employ; it is in agreement with the second law of thermodynamics; and it gives answers which agree with more complete calculations of the expansion.

References

[1]Pergament, H. S. and Calcote, H. F., "Thermal and Chemi-Ionization Processes in Afterburning Rocket Exhausts," *Eleventh Symposium (International) on Combustion*, The Combustion Institution, Pittsburgh, 1967, pp. 597-611.

[2]Mikatarian, R. R., Kau, C. J. and Pergament, H. S., "A Fast Computer Program for Nonequilibrium Rocket Plume Predictions," Air Force Rocket Propulsion Laboratory Technical Report AFRPL-TR-72-94, 1974.

[3]Woodroffe, J. A., "One Dimensional Model for Low Altitude Rocket Exhaust Plumes," AIAA Paper 75-224, Pasadena, Calif., 1975.

[4]Jensen, D. E. and Wilson, A. S., "Prediction of Rocket Exhaust Flame Properties," *Combustion and Flame*, Vol. 25, 1975, pp. 43-55.

[5]Jarvinen, P. O. and Hill, J. A. F., "Universal Model for Underexpanded Rocket Plumes in Hypersonic Flow," presented at 12th JANNAF Liquid Propulsion Meeting, Las Vegas, 1970.

[6]Slattery, J. C., *Momentum, Energy and Mass Transfer in Continua*, Wiley, New York, 1972, Chaps. 4 and 7.

[7]Liepmann, H. W. and Roshko, A., *Elements of Gasdynamics*, Wiley, New York, 1957, p. 20.

[8]Sutton, G. P., *Rocket Propulsion Elements*, Wiley, New York, 1964, pp. 40-41.

[9]Boynton, F. P., Personal communication, Physical Dynamics, Inc., May 1976.

[10]Wilson, K. H., "Discussion of the AFRPL Evaluation of the LMSC-PARL Low Altitude Flowfield Model," Lockheed Missiles and Space Company, Inc., Palo Alto Research Labs Rept. LMSC-D012442, 1976.

Correlation of Turbulent Shear Layer Attachment Peak Heating Near Mach 6

J. Wayne Keyes*
NASA Langley Research Center, Hampton, Va.

Nomenclature

BS, IS, SL	= curved bow shock, plane impinging shock, shear layer, Fig. 1
c_p	= specific heat at constant pressure
d	= body diameter
h	= heat-transfer coefficient
M	= Mach number
p	= static pressure
T	= temperature
u	= velocity
X_{SL}	= total length of shear layer, Fig. 1
$\delta_{SL,T}$	= turbulent shear layer thickness at attachment
θ_{SL}	= shear layer angle relative to local inclination
μ	= viscosity
ρ	= density, $(\rho_w \propto p_p / T_w)$

Subscripts

1, 2, 3, 4, 5	= regions in flowfield, Fig. 1
local	= local value upstream of separation
p	= peak
w, ∞	= wall and freestream, respectively

Introduction

KNOWLEDGE of peak heating in regions of interfering flows, in particular shear layer attachment, is important in the design of components of high-speed vehicles, such as inlet cowl lips, wing and fin leading edges and surface panels, and external protuberances. Investigations of two- and three-dimensional attachment heating were reported in Refs. 1-5. A correlation of free shear layer attachment peak heating on hemispheres was made in Ref. 6.

This Note presents a correlation of new turbulent two-dimensional data and peak heating data for attaching free shear layers from Refs. 3 and 7. The present data were obtained on a 2.54-cm and 5.08-cm-diam cylindrical leading-edge slab 25.4-cm long with widths of 7.62 cm and 10.16 cm, respectively. A sharp leading-edge flat plate (30.48-cm long by 25.4-cm wide) set at 15 and 20 deg was used to generate plane

Received April 25, 1977: revision received July 18, 1977.

Index categories: Boundary Layers and Convective Heat Transfer—Turbulent; Jets, Wakes, and Viscid-Inviscid Flow Interactions; Supersonic and Hypersonic Flow.

*Aerospace Engineer, Fluid Mechanics Branch, High-Speed Aerodynamics Division.

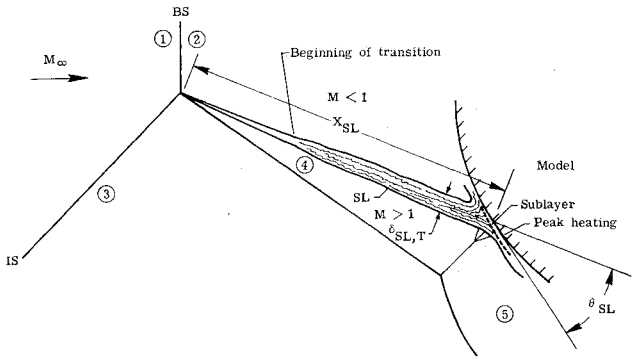

Fig. 1 Sketch of shear layer flowfield.

impinging shocks. The freestream Mach number was 6 with the freestream Reynolds number varying from 3.3×10^6 to 25.6×10^6/m. Peak heating was measured on the silica-based epoxy models using the phase change coating technique.[7,8]

A sketch of the shock pattern for shear layer attachment heating is shown in Fig. 1. This pattern consists of a plane shock intersecting the curved bow shock of the slab, thus creating a free shear layer with an initial thickness essentially zero (order of the shock thickness) and supersonic flow on one side and subsonic flow on the other side ($u_2/u_4 \simeq 0.28$). The shear layer attaches to or interacts with the boundary layer along a line parallel with the cylindrical leading-edge axis causing high local pressure and heating. If the shear layer angle θ_{SL} exceeds the maximum turning angle for region 5, the shear layer becomes detached, and the pattern changes to the "jet impingement" type of interference heating.[1,2] Heat transfer in the attachment region is strongly dependent on the type of shear layer (laminar, transitional, or turbulent[9]), as well as its state of development (if turbulent[3]).

Data Correlation

Peak heating caused by an attaching free shear layer is analogous to a reattaching separated boundary layer.[2,6] In the present case, correlation parameters proposed in Ref. 10 for reattachment heating on two-dimensional ramps are used. These parameters are based on the assumption that a viscous sublayer is formed downstream of the beginning of reattachment and that peak heating occurs near peak pressure.[10] Peak heating is determined by a simple flat-plate relation with the "length of run" taken from the beginning of reattachment, and the local properties are those after the flow has been turned and compressed (region 5 in Fig. 1). It was further stipulated in Ref. 10 that the local density and viscosity be a function of the wall temperature.

Figure 2 presents a correlation of the measured peak Stanton number, $h_p/(\rho_w\, u_5\, c_p)$, as a function of Reynolds numbers based on the length of the sublayer at attachment, $(\rho_w\, u_5\, \delta_{SL,T})/(\mu_w \sin\theta_{SL})$. Values of ρ_w and μ_w are calculated using the measured peak pressure and wall temperature. The sublayer length is approximately equal to $\delta_{SL,T}/\sin\theta_{SL}$ where the shear layer thickness was calculated from the expression,[6] $\delta_{SL,T} = 0.123\, X_{SL}$. Values of X_{SL} and θ_{SL} were obtained from schlieren photographs. All other necessary flow conditions (u_5 and peak pressure p_5, if not known) can be calculated from available computer codes.[11] The present data are compared with data of Refs. 3 and 7 and the data and correlation of Ref. 10 for reattaching turbulent two-dimensional separated flows. The data of Ref. 10 are for initially "fully" developed turbulent boundary layers before separation (turbulent separated flows), whereas the free shear layer data are initially laminar. A comparison of the free shear layer data with the transition data of Ref. 9 indicates that the shear layer data are turbulent at attachment. In general, most of the data fall (a factor of 2) above the data and correlation of Ref. 10. Any effect of attachment angle on

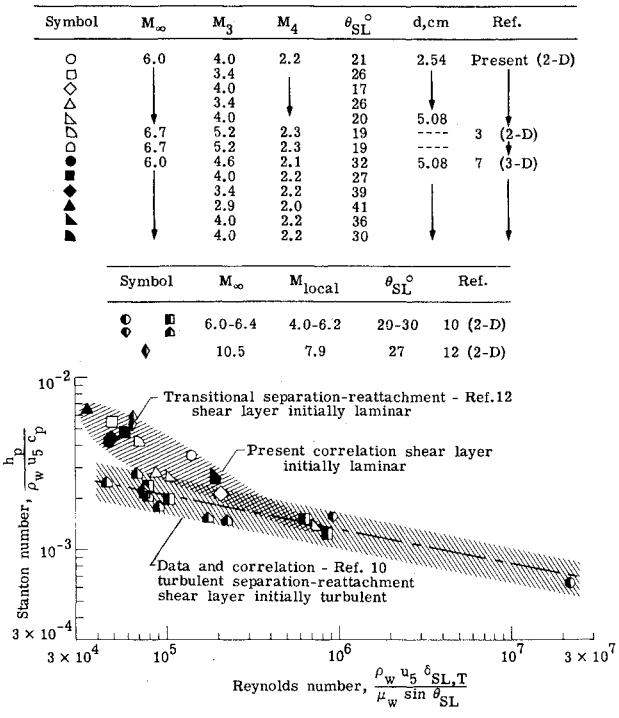

Fig. 2 Correlation of attachment peak heating for shear layers.

heating or any difference between two- and three-dimensional data fall within the data scatter. Also, any differential effect of surface curvature on heating is probably of second order and not significant, because the attaching free shear layers are slightly curved themselves before attaching to the surface of both the two- and three-dimensional models.

The trend of the data indicates that peak heating is strongly influenced by the state of development at attachment. As the free shear layers become more "fully" developed, the data approach the two-dimensional correlation. A tentative explanation is that the free shear layers undergo transition before attachment and, even for Reynolds numbers considerably in excess of the nominal transition value ($\simeq 10^4$),[9] still exhibit a memory or history of the transitional structures. As a check, data from transitional separated flows[12] are shown in Fig. 2, and these data agree with the free shear layer results. This evident persistence of the transitional flow structures has been previously isolated and identified, for example, see Fig. 2 of Ref. 13 for subsonic free flows and Figs. 1 and 2 of Ref. 14 for supersonic/hypersonic boundary-layer case. The research discussed here indicates a similar behavior for supersonic free shear flows also.

References

[1] Edney, B., "Anomalous Heat Transfer and Pressure Distribution on Blunt Bodies at Hypersonic Speeds in the Presence of an Impinging Shock," The Aeronautical Research Institute of Sweden, Stockholm, Sweden, FFA Rept. 115, 1968.

[2] Keyes, J.W. and Hains, F.D., "Analytical and Experimental Studies of Shock Interference Heating in Hypersonic Flows," NASA TN D-7139, 1973.

[3] Birch, S.F. and Rudy, D.H., "Mean Flow Field and Surface Heating Produced by Unequal Shock Interactions at Hypersonic Speeds," NASA TN D-8092, 1975.

[4] Craig, R.R. and Ortwerth, J.O., "Experimental Study of Shock Impingement on a Blunt Leading Edge With Application to Hypersonic Inlet Design," U.S. Air Force, AFAPL-TR-71-10, 1971.

[5] Ginoux, J.J. and Matthews, R.D., "Effect of Shock Impingement on Heat Transfer. Part II: Effect of Shear Layer Impingement on Pressure and Heat Transfer Rate Distributions Around a Cylinder," VKI TN-96-Pt. II, U.S. Air Force Office of Scientific Research, AFOSR-2147-71, Feb. 1974.

[6] Keyes, J.W. and Morris, D.J., "Correlation of Peak Heating in Shock Interference Regions at Hypersonic Speeds," *Journal of Spacecraft and Rockets,* Vol. 9, Aug. 1972, pp. 621-623.

[7] Keyes, J.W., "Shock Interference Peak Heating Measurements Using Phase Change Coatings," *Journal of Spacecraft and Rockets,* Vol. 13, Jan. 1976, pp. 61-63.

[8] Jones, R.A. and Hunt, J.L., "Use of Fusible Temperature Indicators for Obtaining Quantitative Aerodynamic Heat-Transfer Data," NASA TR 4-230, 1966.

[9] Birch, S.F. and Keyes, J.W., "Transition in Compressible Free Shear Layers," *Journal of Spacecraft and Rockets,* Vol. 9, Aug. 1972, pp. 623-624.

[10] Bushnell, D.M. and Weinstein, L.M., "Correlation of Peak Heating for Reattachment of Separated Flows," *Journal of Spacecraft and Rockets,* Vol. 5, Sept. 1968, pp. 1111-1112.

[11] Morris, D.J. and Keyes, J.W., "Computer Programs for Predicting Supersonic and Hypersonic Interference Flow Fields and Heating," NASA TM X-2725, 1973.

[12] Hamilton, H.H. and Dearing, J.D., "Effect of Hinge-Line Bleed on Heat Transfer and Pressure Distribution Over a Wedge-Flap Combination at Mach 10.4," NASA TN D-4686, 1968.

[13] Birch, S.F. and Eggers, J.M., "A Critical Review of the Experimental Data for Developed Free Turbulent Shear Layers," NASA SP-321, 1972.

[14] Bushnell, D.M., Cary, A.M. Jr., and Holley, B.B., "Mixing Length in Low Reynolds Number Compressible Turbulent Boundary Layers," *AIAA Journal,* Vol. 13, Aug. 1975, pp. 1119-1121.

Higher Order Theory for Vibrations of Thick Plates

A. V. Krishna Murty*
Indian Institute of Science, Bangalore, India

THE thick plate is basically a three-dimensional problem. The advantages of being able to treat it as a two-dimensional problem attracted research workers in the past to develop two-dimensional models for the analysis of thick plates. In 1945, Reissner[1] brought out that secondary effects such as transverse shear deformation can assume considerable significance in the bending analysis of elastic plates. In 1951, Mindlin[2] gave a theory for vibration analysis of plates, including the effects of transverse shear and rotary inertia. This formulation involved an unknown coefficient, which was determined by comparison with Lamb's exact solution for an infinite plate. Narasimha Murthy[3] developed an alternate formulation without involving any unknown constant. More recently, Srinivas[4] has carried out extensive studies of thickness effects on vibrations of plates. These studies have shown that, in certain ranges of the parameters involved, application of thin-plate theory can lead to significant errors in the prediction of the frequency spectrum. Thus, there is a need for a theoretical model, with flexibility for incorporating the required level of refinement and some guidelines for the choice of the level of refinement. In this Note, one such theory is presented. Starting from three-dimensional equations of motion, a hierarchy of sets of two-dimensional equations of motion representing the thick-plate behavior to different degrees of approximation have been derived. This derivation proceeds somewhat on similar lines followed by the author in Refs. 5-7 for the case of vibrations of short beams.

Formulation

In a homogeneous, linearly elastic thick plate the three displacement U, V, and W are, in general, functions of x, y, and z. It will be possible to construct a two-dimensional model, if the displacements U, V, and W can be expressed in terms of the midplane displacement u, v, and w and other generalized displacements which depend on x and y. This can be done by adopting the general approach of Ref. 5 with one difference. As in Ref. 5, if the transverse deflection is considered as a sum of two components w_b and w_s, one part w_b corresponding to the classical bending and the second part w_s corresponding to a shear strain which is constant across the thickness, then the second part w_s gives rise to nonzero complementary shear stresses at the top and bottom surfaces of the plate. This results in violation of the stress-free surface conditions and therefore the second component w_s cannot be included. U, V, W, are taken in terms of the midplane displacements u, v, w, as

$$U = u - z\frac{\partial w}{\partial x} + \sum_{n=1,2,3,\ldots} p_n \emptyset_n \tag{1a}$$

$$V = v - z\frac{\partial w}{\partial y} + \sum_{n=1,2,3,\ldots} p_n \psi_n \tag{1b}$$

$$W = w \tag{1c}$$

The midplane displacements u, v, and w and $\emptyset_n$ and ψ_n functions depend upon x and y only. Second terms in the expressions for U and V, correspond to the classical bending of thin plates. $\emptyset_n$, ψ_n terms are included in order to provide for arbitrary variation of U and V across the thickness. Thickness-wise variation of W is ignored as its effect is small on transverse natural frequencies.

As the primary interest here is in the bending vibrations of thick plates, U and V are considered to be antisymmetric in z. Hence $p_n = 0$ at $z = 0$. At the free surfaces $z = \pm t/2$, the shear stress is zero, $dp_n/dz = 0$. To satisfy these conditions p_n are chosen as

$$p_n = \xi^{2n+1} - \frac{2n+1}{2^{2n}}\xi, \quad n = 1,2,3,\ldots,\infty \tag{2}$$

where $\xi = z/t$.

Introducing Eqs. (1) and (2) in the standard three-dimensional stress-strain and strain-displacement relationships, and using the Hamilton principle, the governing equations for transverse vibrations may be deduced as

$$\lambda I\left[\frac{\partial^4 w}{\partial x^4} + 2(\mu+2g)\frac{\partial^4 w}{\partial y^2 \partial x^2} + \frac{\partial^4 w}{\partial y^4}\right] + \rho A\frac{\partial^2 w}{\partial t^2} - \rho I\left[\frac{\partial^4 w}{\partial x^2 \partial t^2} + \frac{\partial^4 w}{\partial y^2 \partial t^2}\right] + \sum_{n=1,2,3,\ldots}^{M}\left[\lambda P_n\left\{\frac{\partial^3 \emptyset_n}{\partial x^3} + \frac{\partial^3 \psi_n}{\partial y^3} + (\mu+2g)\left(\frac{\partial^3 \emptyset_n}{\partial x \partial y^2} + \frac{\partial^3 \psi_n}{\partial y \partial x^2}\right)\right\} - \rho P_n\left(\frac{\partial^3 \psi_n}{\partial y \partial t^2} + \frac{\partial^3 \emptyset_n}{\partial x \partial t^2}\right)\right] = R(x,y,t) \tag{3}$$

$$\lambda P_m\left[\frac{\partial^3 w}{\partial x^3} + (\mu+2g)\frac{\partial^3 w}{\partial x \partial y^2}\right] - \rho P_m\frac{\partial^3 w}{\partial x \partial t^2} + \sum_{n=1,2,\ldots}^{M}\left\{\lambda E_{mn}\left[\frac{\partial^2 \emptyset_n}{\partial x^2} + g\frac{\partial^2 \emptyset_n}{\partial y^2} + (\mu+g)\frac{\partial^2 \psi_n}{\partial x \partial y}\right] - \lambda g S_{mn}\emptyset_n - \rho E_{mn}\frac{\partial^2 \emptyset_n}{\partial t^2}\right\} = 0, \quad m = 1,2,3,\ldots,M \tag{4}$$

Received May 18, 1977; revision received Aug. 11, 1977.
Index categories: Vibration; Structural Dynamics.
*Associate Professor, Dept. of Aeronautical Engineering.